

1 **Generation of thyroid tissues from embryonic stem cells via blastocyst complementation *in vivo***

2
3 Qingsong Ran¹, Qiliang Zhou^{1 *}, Kanako Oda², Akihiro Yasue³, Manabu Abe⁴, Xulu Ye¹, Yingchun Li^{1, 5},
4 Toshikuni Sasaoka², Kenji Sakimura⁴, Yoichi Ajioka⁶, Yasuo Saijo¹

5
6 1) Department of Medical Oncology, 6) Division of Molecular and Diagnostic Pathology, Niigata
7 University Graduate School of Medical and Dental Sciences, Niigata, Japan.

8 2) Department of Comparative and Experimental Medicine, 4) Department of Animal Model
9 Development, Brain Research Institute, Niigata University, Niigata, Japan.

10 3) Department of Orthodontics and Dentofacial Orthopedics, Institute of Biomedical Sciences, Tokushima
11 University Graduate School, Tokushima, Japan.

12 5) Current address: Department of Hematology, Shengjing Hospital of China Medical University,
13 Shenyang, China.

14
15 ***Correspondence:**

16 Qiliang Zhou : zhouql@med.niigata-u.ac.jp

17
18 **The number of words:** 2872

19 **The number of figures and tables:** 4 figures and 0 table.

35 Abstract

36 The generation of mature, functional, thyroid follicular cells from pluripotent stem cells would potentially
37 provide a therapeutic benefit for patients with hypothyroidism, but *in vitro* differentiation remains difficult.
38 We earlier reported the *in vivo* generation of lung organs via blastocyst complementation in fibroblast
39 growth factor 10 (*Fgf10*), compound, heterozygous mutant (*Fgf10* Ex1^{mut}/Ex3^{mut}) mice. *Fgf10* also plays
40 an essential role in thyroid development and branching morphogenesis but any role thereof in thyroid
41 organogenesis remains unclear. Here, we report that the thyroids of *Fgf10* Ex1^{mut}/Ex3^{mut} mice exhibit
42 severe hypoplasia and we generate thyroid tissues from mouse embryonic stem cells (ESCs) in *Fgf10*
43 Ex1^{mut}/Ex3^{mut} mice via blastocyst complementation. The tissues were morphologically normal and
44 physiologically functional. The thyroid follicular cells of *Fgf10* Ex1^{mut}/Ex3^{mut} chimeric mice were derived
45 largely from GFP-positive mouse ESCs although the recipient cells were mixed. Thyroid generation *in*
46 *vivo* via blastocyst complementation will aid functional thyroid regeneration.

47

48 **Keywords:** blastocyst complementation; embryonic stem cells; *Fgf10*; pluripotent stem cells; thyroid
49 generation

50

51 Introduction

52 Continuous, oral thyroid hormone replacement therapy is indispensable for patients with hypothyroidism
53 caused by total thyroidectomy or etiological factors. Although this is relatively simple, effective, safe,
54 and inexpensive, it can be difficult to maintain the complex homeostatic interactions of various
55 hormones^{1, 2}, and the side-effects of over-replacement include cardiac events and osteoporosis also
56 cannot be ignored^{2, 3}. Regeneration and transplantation of thyroid tissue to physiologically supplement
57 thyroid hormone levels is an alternative (radical) treatment strategy^{4, 5}. Derivation of thyroid follicular
58 cells via directed differentiation of pluripotent stem cells (PSCs) *in vitro*, using growth factor-
59 supplemented media, failed to regenerate mature thyroid follicular cells expressing the full genetic suite
60 required for functional thyroid hormone biosynthesis⁶⁻¹⁰. Using an embryonic stem cell (ESC) line
61 hosting a GFP reporter-linked cDNA targeting the locus encoding the homeodomain-containing thyroid
62 transcription factor 1 (TTF1 or *Nkx2-1*), Kurmann et al. reported the generation of functional thyrocytes
63 via activation of bone morphogenetic protein (Bmp) and fibroblast growth factor (Fgf) signaling *in vitro*¹¹.
64 Alternatively, transient forced overexpression of the transcription factors TTF1 and Paired box gene 8
65 (*Pax8*) of mouse or human ESCs allowed the cells to differentiate into functional thyroid follicular cells
66 *in vitro*¹²⁻¹⁵. However, the problems associated with *in vitro* generation of mature thyroid follicular tissue
67 from PSCs, including low differentiation efficiency, the need for genetic labeling to sort and enrich
68 progenitors, and the risk of tumor formation from undifferentiated PSCs after transplantation, limit the
69 clinical applications of cell therapy.

70 Recently, *in vivo* models of organ generation via blastocyst complementation have shown promise.
71 Generation of the pancreas^{16, 17}, kidney^{18, 19}, blood vasculature²⁰ and lung²¹ via intra- or inter-species
72 blastocyst complementation have been reported. Very recently, we used fibroblast growth factor 10,
73 (*Fgf10*), compound, heterozygous mutant (*Fgf10* Ex1^{mut}/Ex3^{mut}) mice to generate lungs via blastocyst
74 complementation²². *Fgf10* Ex1^{mut}/Ex3^{mut} mice exhibited limb and lung deficiencies, as did *Fgf10* Ex1 -/-
75 and *Fgf10* Ex3 -/- mice, as well as other *Fgf10*-knockout mice²³⁻²⁵. Complementation with ESCs enabled
76 *Fgf10* Ex1^{mut}/Ex3^{mut} mice to survive to adulthood without any abnormality.

77 In contrast to the relatively distinct role played by *Fgf10* in lung development and branching
78 morphogenesis^{23, 24, 26-28}, indefiniteness remains in thyroid organogenesis. Thyroid agenesis has been
79 reported in mice deficient in *Fgf10*²⁴ or its receptor *Fgfr2b*²⁹, indicating that *Fgf10*-*Fgfr2b* signaling plays
80 a crucial role in thyroid organogenesis. However, although the thyroid primordium was absent at E13, the
81 stage at which thyroid morphogenesis was impaired was not explored. *Nkx2-1*⁺/*Sox 9*⁺ thyroid progenitors
82 were detected in the thyroid placode at E9.5; weak expression of *Fgfr2b* in the thyroid primordium at
83 E12.5; and distinct expression of *Fgf10* in the mesenchyme at E15.5³⁰. By contrast, it has been reported
84 that *Fgf10*-null mutant mouse embryos did not exhibit thyroid agenesis but rather severe hypoplasia (the
85 thyroid was shaped normally)^{30, 31}. Similarly, conditional knockout of *Fgf10* (*Wnt1cre Fgf10* fl/fl) in
86 neural crest, from which several head tissues are derived (including the mesenchyme around the
87 developing thyroid glands), resulted thyroid remnants³¹. Therefore, we explored the thyroid phenotype of
88 *Fgf10* Ex1^{mut}/Ex3^{mut} mice and the possibility of thyroid generation in such mice from PSCs (thus via
89 blastocyst complementation).

90 Here, we report that the thyroids of *Fgf10* Ex1^{mut}/Ex3^{mut} mice are normally shaped but severely
91 hypoplastic. Complementation with ESCs rescued thyroid organogenesis. Generation of thyroids *in vivo*
92 via blastocyst complementation will aid functional thyroid regeneration.

93 **Materials and Methods**

94 ***Generation of Fgf10 Ex1^{mut}/Ex3^{mut} mice and chimeric mice***

95 All animal experiments were approved by the Institutional Animal Care and Use Committee of Niigata
96 University, Niigata, Japan (approval number SA00233). *Fgf10* Ex1^{wild/mut} and *Fgf10* Ex3^{wild/mut} mice were
97 generated using the CRISPR/Cas9 system as described in our previous report²². *Fgf10* Ex1^{mut}/Ex3^{mut} mice
98 were obtained by intercrossing *Fgf10* Ex1^{wild/mut} mice with *Fgf10* Ex3^{wild/mut} mice. Generation of *Fgf10*
99 Ex1^{mut}/Ex3^{mut} chimeric mice via blastocyst complementation proceeded as described previously²². Briefly,
100 embryos were prepared via *in vitro* fertilization of *Fgf10* Ex3 -/+ ova with *Fgf10* Ex1 -/+ sperm, and five
101 to eight GFP-expressing mouse RENKA C57BL/6NCr1Crlj ESCs (#CFS-EGFP27; Brain Research
102 Institute, Niigata University) were prepared and microinjected into the perivitelline space of eight-
103 cell/morula-stage embryos. After further culture *in vitro*, the embryos were transferred into the uteri of

104 pseudopregnant, recipient ICR female mice. Genotyping of the *Fgf10* Ex1^{mut}/Ex3^{mut} mice and chimeric
105 mice were performed using the Surveyor System and DNA sequencing, as described previously²².

106 ***Histological analysis***

107 Mouse tissues were fixed in 10% (v/v) neutral buffered formalin, embedded in paraffin, sectioned, and the
108 sections deparaffinized with xylene and hydrated in a graded series of ethanol baths. Hematoxylin and
109 eosin (H&E) and immunofluorescence staining were performed as described previously²². The primary
110 antibodies were anti-GFP polyclonal antibody (goat IgG, 1:200; #GTX26673; GeneTex, Irvine, CA,
111 USA); anti-TTF1 monoclonal antibody (rabbit IgG, 1:200; #ab76013; Abcam, Cambridge, UK); anti-
112 FOXE1 polyclonal antibody (rabbit IgG, 1:200; #bs-0446r; Bioss, Woburn, MA, USA); anti-Pax8
113 antibody (rabbit IgG, 1:200; #10337-1-AP; Proteintech, Chicago, IL, USA); anti-thyroglobulin
114 monoclonal antibody (rabbit IgG, 1:200; #ab156008; Abcam); anti-T3 polyclonal antibody (rabbit IgG,
115 1:200; #MBS2001953; MyBioSource, San Diego, CA, USA); anti-calcitonin polyclonal antibody (rabbit
116 IgG, 1:200; #GTX134005; GeneTex); anti-vimentin monoclonal antibody (rabbit IgG, 1:200; #ab92574;
117 Abcam); and anti-Ki-67 polyclonal antibody (rabbit IgG, 1:200; #ab15580, Abcam). Donkey anti-goat
118 IgG-Alexa Fluor 488 (1:200; #A11055; Invitrogen, Carlsbad, CA, USA) and donkey anti-rabbit IgG-
119 Alexa Fluor 594 (1:200; #A21207; Invitrogen) served as secondary antibodies. Nuclei were counterstained
120 with 4',6-diamidino-2-phenylindole (DAPI) and fluorescence images acquired using a C1si confocal
121 microscope (Nikon, Tokyo, Japan).

122 TTF1-positive cells were counted in over 1,500 cells in at least three images (200× magnification)
123 randomly selected from the thyroids of each mouse. GFP-positive cells among TTF1-positive cells were
124 counted and the percentage of GFP/TTF1-positive cells was then calculated.

125 ***Contrast-enhanced micro-computed tomography (CT)***

126 To explore the macroscopic phenotypes of the thyroid tissues of *Fgf10* Ex1^{mut}/Ex3^{mut} neonatal mice and
127 *Fgf10* Ex1^{mut}/Ex3^{mut} chimeric neonatal mice, contrast-enhanced micro-CT analysis was performed as
128 described previously²² with slight modifications. Briefly, neonatal mice were first fixed in 4% (v/v)
129 paraformaldehyde at 4°C for 2 days. A midline cervical incision was then created and the larynx, trachea
130 and thyroid exposed. Then, the mice were immersed in 25% (v/v) Lugol's iodine solution at room
131 temperature for 5 days. Subsequently, the samples were scanned using a micro-CT device (Nittetsu Elex,
132 Tokyo, Japan) and the data analyzed with the aid of TRI/3D-Bon software (Ratoc System Engineering Co.
133 Ltd., Tokyo, Japan).

134 ***Enzyme-linked immunosorbent assays (ELISA)***

135 Serum tri-iodothyronine (T3) and thyroxine (T4) concentrations were measured using ELISA kits (CSB-
136 E05086m for T3, CSB-E05083m for T4; CUSABIO, Wuhan, China), according to the manufacturer's
137 protocols. Briefly, 50 µL of standards or blood samples were added to 96-well plates, followed by 50 µL

138 of conjugate reagents; incubation proceeded for 60 min at 37°C. The liquid was aspirated, the wells
139 washed three times, 50 µL of the HRP–avidin reagent added, and the plates incubated for 30 min at 37°C.
140 The liquid was aspirated, the wells washed three times, and 50 µL of substrate A and B added. After
141 incubation for 15 min at 37°C in the dark, 50 µL of stop solution was added and the optical density at 450
142 nm measured within 10 min using a microplate reader. All tests were performed in duplicate.

143 **Statistical analysis**

144 Data are presented as the means ± standard deviations. One-way analysis of variance and the Tukey–
145 Kramer test were used to assess the significance of differences. A *p*-value < 0.05 was deemed to indicate
146 significance.

147

148 **Results**

149 ***Fgf10* Ex1^{mut}/Ex3^{mut} mice exhibit severe thyroid hypoplasia**

150 *Fgf10* Ex1^{mut}/Ex3^{mut} mice were generated as previously reported²². Consistent with the data of a recent
151 study on embryonic growth of the thyroid gland in *Fgf10*-null mutant mice³⁰, neonatal *Fgf10*
152 Ex1^{mut}/Ex3^{mut} mice exhibited bilateral thyroid remnants (Fig. 1A) on micro-CT analysis. Serial sections
153 of the entire glands (n = 5) confirmed that the thyroids were normally shaped but smaller than those of
154 *Fgf10*^{wild/wild} neonates (Supplemental videos 1 and 2). H&E and immunofluorescence staining indicated
155 that the hypoplastic thyroid glands of *Fgf10* Ex1^{mut}/Ex3^{mut} mice had a lower proportion of parenchyma,
156 decreased branching, and fewer follicles than normal mouse thyroids (Figs. 1B and C).
157 Immunofluorescence staining indicated that the number of thyroid cells expressing TTF1 and Pax8 (the
158 most important transcription factors in terms of thyroid gland organogenesis) was decreased in neonatal
159 *Fgf10* Ex1^{mut}/Ex3^{mut} mice compared to neonatal *Fgf10*^{wild/wild} mice (Fig. 1C). Although the protein levels
160 seem to be similar, the total expression levels of thyroglobulin (Tg) (a precursor protein of thyroid
161 hormone) and tri-iodothyronine (T3) were reduced in neonatal *Fgf10* Ex1^{mut}/Ex3^{mut} mice (Fig. 1C). Ki-
162 67 positive proliferating cells were obviously reduced in thyroids of neonatal *Fgf10* Ex1^{mut}/Ex3^{mut} mice
163 compared to neonatal *Fgf10*^{wild/wild} mice (Fig. 1C). The expression of calcitonin in the neonatal *Fgf10*
164 Ex1^{mut}/Ex3^{mut} mice did not seem to decrease significantly (Fig. 1C), in agreement with a previous report
165 that *Fgf10* is not involved in parafollicular cell differentiation³⁰.

166 **Generation of thyroid tissues in *Fgf10* Ex1^{mut}/Ex3^{mut} mice**

167 We next sought to generate thyroid tissues from PSCs in *Fgf10* Ex1^{mut}/Ex3^{mut} mice via blastocyst
168 complementation. Micro-CT confirmed the existence of thyroids adjacent to the trachea at the front of the
169 neck of neonatal *Fgf10* Ex1^{mut}/Ex3^{mut} chimeras; the glands were of normal shape and size (Fig. 1A). The
170 thyroids of *Fgf10* Ex1^{mut}/Ex3^{mut} chimeric neonates (Fig. 1B and Supplemental video 3) were histologically
171 normal (thus similar to those of *Fgf10*^{wild/wild} neonates) (Fig. 1B and Supplemental video 1). The thyroid
172 tissues of *Fgf10* Ex1^{mut}/Ex3^{mut} chimeras exhibited high-level GFP expression compared to those of *Fgf10*

173 ^{wild/wild} neonates (Figs. 1D, E), indicating a major contribution from GFP-expressing mouse ESCs. The
174 levels of TTF1, Tg, and T3 in the thyroids of neonatal *Fgf10* Ex1^{mut}/Ex3^{mut} chimeras (Fig. 1F) were similar
175 to those of neonatal *Fgf10* ^{wild/wild} mice (Fig. 1C). The GFP expression of TTF1-positive follicular cells
176 predominated, but was mosaic; while those of calcitonin-positive parafollicular cells and vimentin -
177 positive stromal cells showed no preponderance (Fig. 1F). These data indicated that thyroid tissues were
178 generated in *Fgf10* Ex1^{mut}/Ex3^{mut} mice via blastocyst complementation.

179 **Characterization of the thyroids of adult *Fgf10* Ex1^{mut}/Ex3^{mut} chimeric mice**

180 We showed that survival of *Fgf10* Ex1^{mut}/Ex3^{mut} mice to adulthood was rescued by complementation with
181 mouse ESCs²². Next, we analyzed the thyroid tissues of five *Fgf10* Ex1^{mut}/Ex3^{mut} adult chimeric mice.
182 We lacked data on adult *Fgf10* Ex1^{mut}/Ex3^{mut} mice because they died immediately after birth; they had no
183 lungs. The low proportion of parenchyma in the thyroids of *Fgf10* Ex1^{mut}/Ex3^{mut} neonates (Fig. 1B)
184 recovered in the thyroid tissues of adult *Fgf10* Ex1^{mut}/Ex3^{mut} chimeras (Fig. 2A). The thyroid follicles of
185 adult *Fgf10* Ex1^{mut}/Ex3^{mut} chimeras were well-organized spheres lined with follicular cells surrounding
186 lumina that contained a colloid, as in adult *Fgf10* ^{wild/wild} mice (Fig. 2A). The thyroid follicular cells of
187 adult *Fgf10* Ex1^{mut}/Ex3^{mut} chimeras expressed TTF1, FOXE1 (formerly TTF2), and Pax8 at levels similar
188 to those of adult *Fgf10* ^{wild/wild} mice (Fig. 2B). Calcitonin-positive parafollicular cells were detected in
189 connective tissue adjacent to the thyroid follicles, as in adult *Fgf10* ^{wild/wild} mice (Fig. 2B). Thus, the
190 thyroids of adult *Fgf10* Ex1^{mut}/Ex3^{mut} chimeric mice were histologically normal.

191 Next, we investigated the contribution of GFP-expressing mouse ESCs to the thyroids. Extremely
192 strong, diffuse, GFP expression across all thyroid tissues was observed in *Fgf10* Ex1^{mut}/Ex3^{mut} adult
193 chimeras compared to adult *Fgf10* ^{wild/wild} mice or *Fgf10* Ex1^{wild}/Ex3^{mut} chimeras (Fig. 2B). In *Fgf10*
194 Ex1^{mut}/Ex3^{mut} adult chimeric mice, large proportions of the TTF1-, FOXE1-, and Pax8-positive follicular
195 cells were GFP-positive, indicating that the cells were derived principally from mouse ESCs (Fig. 2B).
196 The extent of GFP expression in non-follicular regions, including parafollicular cells, blood vessels, and
197 connective tissues, did not differ between the *Fgf10* Ex1^{mut}/Ex3^{mut} and Ex1^{wild}/Ex3^{mut} chimeras (Fig. 2B).
198 Moreover, 86.4 ± 7.9% of follicular cells in adult *Fgf10* Ex1^{mut}/Ex3^{mut} chimeras were derived from GFP-
199 positive mouse ESCs, a greater proportion than in adult *Fgf10* ^{wild/wild} and Ex1^{mut} or Ex3^{mut} chimeras (Fig.
200 2C). Next, we assessed the physiological function of the thyroid tissues of adult *Fgf10* Ex1^{mut}/Ex3^{mut}
201 chimeras. Immunofluorescence staining confirmed cytosolic expression of Tg and deposition thereof in
202 the thyroid follicular lumina (Fig. 3A). T3 was also detected in the colloid, as in adult *Fgf10* ^{wild/wild} mice
203 (Fig. 3A). ELISA confirmed that the plasma T3 and thyroxine (T4) levels of adult *Fgf10* Ex1^{mut}/Ex3^{mut}
204 chimeras were similar to those of adult *Fgf10* ^{wild/wild} mice and Ex1^{mut} or Ex3^{mut} chimeric mice (Fig. 3B).
205 Thus, thyroids of adult *Fgf10* Ex1^{mut}/Ex3^{mut} chimeras were functional. Thus, the functional thyroid
206 follicles were generated principally from mouse ESCs in adult *Fgf10* Ex1^{mut}/Ex3^{mut} chimeric mice, via
207 blastocyst complementation.

209 Discussion

210 We generated thyroid tissues in *Fgf10* Ex1^{mut}/Ex3^{mut} mice with severely hypoplastic thyroids via
211 blastocyst complementation with mouse ESCs. The generated thyroids were morphologically normal and
212 physiologically functional compared to those of *Fgf10*^{wild/wild} mice. The generated thyroid tissues
213 exhibited significant contributions from GFP-positive ESCs but the recipient cells were mixed.

214 Early during mouse thyroid development, thyroid progenitors expressing a specific combination
215 of four critical transcription factors [Nkx2-1, Pax8, FOXE1 (Forkhead Box E1), and HHEX
216 (hematopoietically expressed homeobox)] assemble to form the thyroid bud in the anterior foregut
217 endoderm^{32, 33}. These transcription factors are linked to an integrated regulatory network that controls
218 thyroid survival and migration during organogenesis, via cell-autonomous mechanisms^{32, 33}. Deletion of a
219 gene encoding any of these transcription factors triggers athyreosis or severe thyroid hypoplasia³⁴. *Fgf10*
220 plays essential roles in the development of many organs such as the thyroid, limbs, lungs, and pituitary
221 and salivary glands, mediated principally via the mesenchymal–epithelial interaction signaled through the
222 receptor *Fgfr2-IIIb*^{24, 35}. Mice deficient in *Fgf10* or *Fgfr2b* exhibit athyreosis, indicating that *Fgf10* is
223 required for thyroid budding and branching morphogenesis^{24, 29}. However, a recent study reported that
224 most *Fgf10*-null mouse embryos exhibited small, unilateral remnant thyroids, indicating that
225 organogenesis proceeded even in the complete absence of *Fgf10*³¹. Conditional, neural crest *Fgf10* knock-
226 out reduced thyroid size to a lesser degree than in the null mutant, suggesting that a source of *Fgf10* apart
227 from the neural crest might be available to assist thyroid development³¹. A recent work on thyroid
228 branching morphogenesis showed that normally shaped, symmetrical thyroids were present in *Fgf10*-null
229 mutant mouse embryos, but were severely hypoplastic³⁰. *Fgf10*–*Fgfr2b* signaling may thus be dispensable
230 in terms of thyroid specification and early development, but is required to regulate organogenesis³⁰. We
231 found that the thyroids of neonatal, *Fgf10* compound heterozygous mutant (*Fgf10* Ex1^{mut}/Ex3^{mut}) mice
232 were severely hypoplastic but symmetrically residual, supporting the above observations in mouse
233 embryos^{30, 31}. Furthermore, complementation with *Fgf10* wild-type ESCs rescued thyroid organogenesis
234 both histologically and functionally in *Fgf10* Ex1^{mut}/Ex3^{mut} mice, indicating that *Fgf10* played essential
235 roles in late thyroid development and organogenesis.

236 Although *Fgf10* seems to be dispensable in terms of thyroid specification and early thyroid
237 development, *Fgf10*-induced branching growth has been reported to account for over 80% of thyroid
238 enlargement before birth³⁰. Given the symmetrical, severe thyroid hypoplasia of *Fgf10* Ex1^{mut}/Ex3^{mut} mice,
239 we expected that it might be possible to generate functional thyroid tissues from PSCs in such mice via
240 blastocyst complementation. Indeed, high proportions of the thyroid follicular cells of *Fgf10*
241 Ex1^{mut}/Ex3^{mut} adult chimeric mice were GFP-positive (Fig. 2B), indicating major contributions from
242 donor ESCs. Localized *Fgf10* expression by donor ESCs in the mesenchyme around developing thyroid

243 glands would act non-selectively (via Fgfr2-IIIb-mediated mesenchymal–epithelial interaction signaling)
244 on both GFP-positive donor cells (*Fgf10*^{wild/wild}) and GFP-negative host cells (*Fgf10* Ex1^{mut}/Ex3^{mut})
245 resident in the endoderm. However, other mechanisms [such as ectopic expression of Fgf10 in the GFP-
246 positive donor epithelium (*Fgf10*^{wild/wild}), as indicated during lung generation via blastocyst
247 complementation]²² may explain in the relative preponderance of GFP-positive donor ESCs during thyroid
248 development compared to the level in the *Fgf10* Ex1^{mut}/Ex3^{mut} host epithelium. Importantly, ESC-derived
249 thyroid follicles expressed and deposited T3 as did adult *Fgf10*^{wild/wild} mice (Fig. 3A). These data, together
250 with the ELISA results indicating that adult *Fgf10* Ex1^{mut}/Ex3^{mut} chimeras had normal T3 and T4 plasma
251 levels compared to adult *Fgf10*^{wild/wild} mice (Fig. 3B), indicated that the mature, functional thyroid follicle
252 tissues of adult *Fgf10* Ex1^{mut}/Ex3^{mut} chimeras were generated predominantly from ESCs.

253 Directed *in vitro* differentiation of PSCs using growth factors has been reported, but failed to
254 regenerate mature thyroid follicular cells⁶⁻¹⁰. Derivation of functional thyroid follicular cells *in vitro* from
255 mouse and human induced PSCs^{4, 11}, mouse ESCs^{12, 13, 15}, and human ESCs¹⁴ has been reported using
256 several protocols. However, the generation of such cells from PSCs is inefficient; enrichment and sorting
257 of precursor cells currently requires genetic editing (TTF1 and Pax8 overexpression or labeling of targeted
258 alleles)^{34, 36}. Also, the risk of tumor formation from undifferentiated PSCs on transplantation after *in vitro*
259 differentiation cannot be ignored. Our current work indicates that mature, functional thyroid follicular
260 cells can be generated from PSCs via blastocyst complementation. Although the generated thyroid tissues
261 in *Fgf10* Ex1^{mut}/Ex3^{mut} chimeras were mixtures of donor and host cells, this is not an argument against
262 thyroid regeneration, because transplantation of mature thyroid follicular cells (not the organ) would
263 suffice as therapy for patients with hypothyroidism. Sorting of PSC-derived mature follicular cells or
264 follicular tissues is required. Furthermore, the low efficiency of adult *Fgf10* Ex1^{mut}/Ex3^{mut} chimera
265 generation (5 adult compound heterozygous chimeras weaned from 76 neonatal chimeras obtained by
266 transplantation of 638 blastocysts)²² and the undesirable thyroid chimerism of the present study require
267 attention. The use of a conditional knockout method or other knockout targets such as Nkx2-1, Pax8, or
268 Fgf2 (all of which are essential for early thyroid development) might be useful. Wen *et al.* recently
269 generated lung and thyroid epithelial cell lineages almost entirely from mouse ESCs in Nkx2-1 knockout
270 mice via blastocyst complementation³⁷. Exploring the possibility of generation of PSC-derived thyroid
271 tissues via inter-species blastocyst complementation in rodents or livestock remains to be investigated²².
272 Another concern is that human PSCs-derived cells will appear in the brains and gonads of livestock,
273 especially when generating human organs from PSCs in livestock using the current inter-species blastocyst
274 complementation technique. The use of committed stem or progenitor cells, or PSCs genetically modified
275 to restrict their differentiation potential, would address this issue¹⁶, but clinical application remains some
276 way off.

277 In summary, we showed that *Fgf10* played an essential role in thyroid development and that thyroid
278 tissues generated in thyroid hypoplastic *Fgf10* Ex1^{mut}/Ex3^{mut} mice were largely derived from mouse ESCs
279 via blastocyst complementation. Generation of PSC-derived thyroid tissues via blastocyst
280 complementation is a promising approach to thyroid regeneration.

281281

282 ***Conflict of interest statement***

283 No author has any conflict of interest.

284284

285 **Author contributions**

286 Qingsong Ran performed experiments, contributed to data analysis and interpretation, and assisted with
287 manuscript preparation. Kanako Oda and Toshikuni Sasaoka performed the embryo manipulation and
288 animal experiments, and contributed to the analysis and interpretation of mouse data. Akihiro Yasue
289 generated the *Fgf10* knockout mouse and contributed to DNA analysis. Manabu Abe and Kenji Sakimura
290 prepared the GFP-positive mouse ESCs and assisted with embryo manipulation. Xulu Ye and Yingchun
291 Li performed some of the experiments. Yoichi Ajioka contributed to histological analysis and sequencing.
292 Yasuo Saijo and Qiliang Zhou designed the project, performed some of the experiments, analyzed the data,
293 and wrote the manuscript. All authors have discussed the results and commented on the manuscript.

294294

295 **Funding**

296 This work was supported in part by the Japan Society for the Promotion of Science (KAKENHI; grant
297 nos. 18K15921 and 18H02817G).

298

299 **Acknowledgments**

300 We thank Takenori Sakuma, Nae Saito, and Sumika Uchiyama for assistance with embryo manipulation,
301 mouse housing, and mouse tissue sampling. We thank Rie Natsume for assistance with embryo micro-
302 injection, and Shinichi Kenmotsu and Hayato Ohshima for assistance with micro-CT.

303303

304 **References**

- 305 1. Arauchi A, Shimizu T, Yamato M, Obara T, Okano T. (2009). Tissue-engineered thyroid cell sheet
306 rescued hypothyroidism in rat models after receiving total thyroidectomy comparing with
307 nontransplantation models. *Tissue Eng Part A*. 15(12), 3943-3949.
- 308 2. Yang Y, Opara EC, Liu Y, Atala A, Zhao W. (2017). Microencapsulation of porcine thyroid cell
309 organoids within a polymer microcapsule construct. *Exp Biol Med* (Maywood). 242(3):286-296.
- 310 3. Clarke N, Kabadi UM. (2004). Optimizing treatment of hypothyroidism. *Treat Endocrinol*. 3, 217-21

- 311 4. Arauchi A, Matsuura K, Shimizu T, Okano T. (2017). Functional Thyroid Follicular Cells
312 Differentiation from Human-Induced Pluripotent Stem Cells in Suspension Culture. *Front Endocrinol*
313 (Lausanne). 8, 103.
- 314 5. Huang Y, Yamanouchi K, Sakai Y, et al. (2019). Fabrication of Functional Cell Sheets with Human
315 Thyrocytes from Non-Tumorous Thyroid Tissue. *Tissue Eng Regen Med.* 16(5), 491-499.
- 316 6. Arufe MC, Lu M, Kubo A, Keller G, Davies TF, Lin RY. (2006). Directed differentiation of mouse
317 embryonic stem cells into thyroid follicular cells. *Endocrinology.* 147, 3007–3015.
- 318 7. Arufe MC, Lu M, Lin RY. (2009). Differentiation of murine embryonic stem cells to thyrocytes
319 requires insulin and insulin-like growth factor-1. *Biochem Biophys Res Commun.* 381, 264–270.
- 320 8. Ma R, Latif R, Davies TF. (2009). Thyrotropin-independent induction of thyroid endoderm from
321 embryonic stem cells by activin A. *Endocrinology.* 150, 1970–1975.
- 322 9. Jiang N, Hu Y, Liu X, et al. (2010). Differentiation of E14 mouse embryonic stem cells into thyrocytes
323 in vitro. *Thyroid.* 20, 77–84.
- 324 10. Longmire TA, Ikonomou L, Hawkins F, et al. (2012). Efficient derivation of purified lung and thyroid
325 progenitors from embryonic stem cells. *Cell Stem Cell.* 10, 398–411.
- 326 11. Kurmann AA, Serra M, Hawkins F, et al. (2015). Regeneration of Thyroid Function by
327 Transplantation of Differentiated Pluripotent Stem Cells. *Cell Stem Cell.* 17(5), 527-542.
- 328 12. Antonica F, Kasprzyk DF, Opitz R, et al. (2012). Generation of functional thyroid from embryonic
329 stem cells. *Nature.* 491, 66–71.
- 330 13. Ma R, Latif R, Davies TF. (2013). Thyroid follicle formation and thyroglobulin expression in
331 multipotent endodermal stem cells. *Thyroid.* 23, 385–391.
- 332 14. Ma R, Latif R, Davies TF. (2015). Human embryonic stem cells form functional thyroid follicles.
333 *Thyroid.* 25(4), 455-461.
- 334 15. Dame K, Cincotta S, Lang AH, et al. (2017). Thyroid Progenitors Are Robustly Derived from
335 Embryonic Stem Cells through Transient, Developmental Stage-Specific Overexpression of Nkx2-1.
336 *Stem Cell Reports.* 8(2), 216-225.
- 337 16. Kobayashi T, Yamaguchi T, Hamanaka S, et al. (2010). Generation of rat pancreas in mouse by
338 interspecific blastocyst injection of pluripotent stem cells. *Cell.* 142, 787–799.
- 339 17. Yamaguchi T, Sato H, Kato-Itoh M. et al. (2017). Interspecies organogenesis generates autologous
340 functional islets. *Nature.* 542, 191–196.
- 341 18. Usui J, Kobayashi T, Yamaguchi T. et al. (2012). Generation of kidney from pluripotent stem cells
342 via blastocyst complementation. *Am. J. Pathol.* 180, 2417–2426.
- 343 19. Teppei G, Hiromasa H, Makoto S, et al. (2019). Generation of pluripotent stem cell-derived mouse
344 kidneys in Sall1-targeted anephric rats. *Nat Commun.* 10, Article number: 451.
- 345 20. Wang X, Shi H, Zhou J, et al. (2020). Generation of rat blood vasculature and hematopoietic cells in

346 rat-mouse chimeras by blastocyst complementation. *J Genet Genomics*. May 19, S1673-
347 8527(20)30086-2.

348 21. Mori M, Furuhashi K, Danieleson JA, et al. (2019). Generation of functional lungs via conditional
349 blastocyst complementation using pluripotent stem cells. *Nat Med*. 25, 1691-1698.

350 22. Kitahara A, Ran Q, Oda K, et al. (2020). Generation of Lungs by Blastocyst Complementation in
351 Apneumatic Fgf10-Deficient Mice. *Cell Rep*. 31(6), 107626.

352 23. Sekine K, Ohuchi H, Fujiwara M, et al. (1999). Fgf10 is essential for limb and lung formation. *Nat*
353 *Genet*. 21, 138-141.

354 24. Ohuchi H, Hori Y, Yamasaki M, et al. (2000). FGF10 acts as a major ligand for FGF receptor 2
355 IIIb in mouse multi-organ development. *Biochem. Biophys. Res. Commun*. 277, 643-9.

356 25. Yasue A, Mitsui S, Watanabe T. et al. (2014). Highly efficient targeted mutagenesis in one-cell mouse
357 embryos mediated by the TALEN and CRISPR/Cas systems. *Sci. Rep*. 4, 5705.

358 26. Bellusci S, Grindley J, Emoto H, Itoh N, Hogan BL. (1997). Fibroblast growth factor 10 (FGF10)
359 and branching morphogenesis in the embryonic mouse lung. *Development*. 124(23), 4867-78.

360 27. Abler LL, Mansour SL, Sun X. (2009). Conditional gene inactivation reveals roles for Fgf10 and
361 Fgfr2 in establishing a normal pattern of epithelial branching in the mouse lung. *Dev Dyn*. 238(8),
362 1999-2013.

363 28. Yuan T, Volckaert T, Chanda D, Thannickal VJ, De Langhe SP. (2018). Fgf10 signaling in lung
364 development, homeostasis, disease, and repair after injury. *Front. Genet*. 9, 418.

365 29. Revest J M, Spencer-Dene B, Kerr K, De Moerlooze L, Rosewell I and Dickson C. (2001). Fibroblast
366 growth factor receptor 2-IIIb acts upstream of Shh and Fgf4 and is required for limb bud maintenance
367 but not for the induction of Fgf8, Fgf10, Msx1, or Bmp4. *Dev. Biol*. 231, 47-62.

368 30. Liang S, Johansson E, Barila G, Altschuler DL, Fagman H, Nilsson M. (2018). A branching
369 morphogenesis program governs embryonic growth of the thyroid gland. *Development*. 145(2),
370 dev146829.

371 31. Teshima TH, Lourenco SV, Tucker AS. (2016). Multiple cranial organ defects after conditionally
372 knocking out Fgf10 in the neural crest. *Front Physiol*. 7, 488.

373 32. Parlato R, Rosica A, Rodriguez-Mallon A, et al. (2004). An integrated regulatory network controlling
374 survival and migration in thyroid organogenesis. *Dev Biol*. 276, 464-475.

375 33. Fagman H, Nilsson M. (2011). Morphogenetics of early thyroid development, *J. Mol. Endocrinol*.
376 46(1), R33-R42.

377 34. Nilsson M, Fagman H. (2017). Development of the thyroid gland. *Development*. 144, 2123-2140.

378 35. Itoh N. (2016). Fgf10: a multifunctional mesenchymal-epithelial signaling growth factor in
379 development, health, and disease. *Cytokine Growth Factor Rev*. 28, 63-69

380 36. Hollenberg AN, Choi J, Serra M, Kotton DN. (2017). Regenerative therapy for hypothyroidism:

381 Mechanisms and possibilities. *Mol Cell Endocrinol.* 445, 35-41.
382 37. Wen B, Li E, Ustiyani V, et al. (2020). In Vivo Generation of Lung and Thyroid Tissues from
383 Embryonic Stem Cells using Blastocyst Complementation. *Am J Respir Crit Care Med.* Sep 2. doi:
384 10.1164/rccm.201909-1836OC. Online ahead of print.

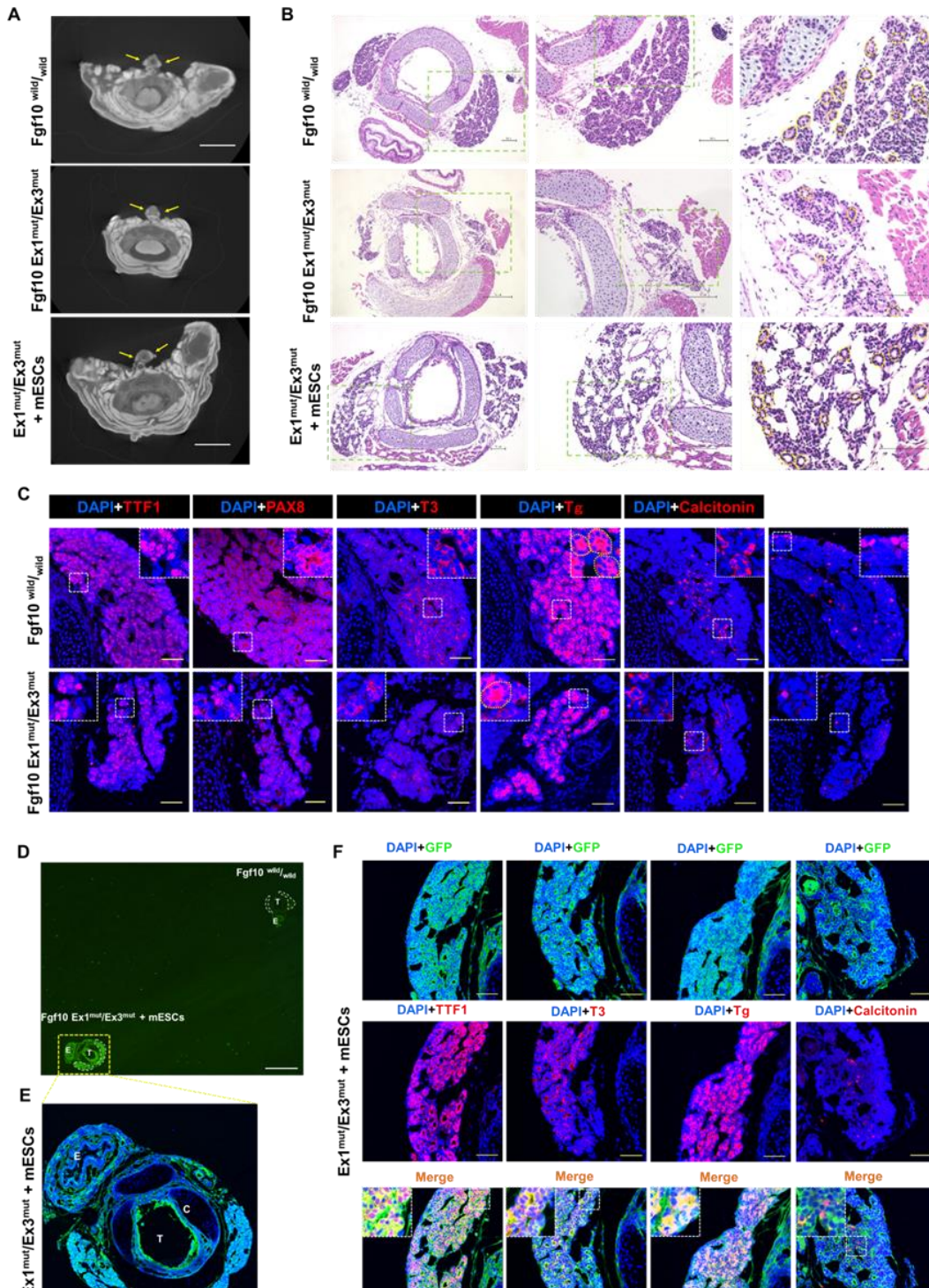


Figure 1. Characterization of the thyroids of *Fgf10* $Ex1^{mut}/Ex3^{mut}$ neonates and $Ex1^{mut}/Ex3^{mut}$ chimeric neonates complemented with mouse embryonic stem cells (mESCs). **A:** Axial micro-computed tomography images of the neck regions of *Fgf10*^{wild/wild} and $Ex1^{mut}/Ex3^{mut}$ neonates and $Ex1^{mut}/Ex3^{mut}$ chimeric neonates. Yellow arrows indicate thyroid lobes adjacent to the tracheae. Scale bar = 2 mm. **B:** Hematoxylin and eosin staining of cervical cross-sections of *Fgf10*^{wild/wild} and $Ex1^{mut}/Ex3^{mut}$ neonates and $Ex1^{mut}/Ex3^{mut}$ chimeric neonates. The right panels show magnified views of the areas indicated by the green dotted lines in the left panels. Scale bars = 100 μ m. **C:** Immunofluorescence staining of the thyroids of *Fgf10*^{wild/wild} and $Ex1^{mut}/Ex3^{mut}$ neonates for various markers (red): TTF1, thyroid transcription factor 1; PAX8, paired box gene 8; T3, tri-iodothyronine; Tg, thyroglobulin; Calcitonin and Ki-67. Nuclei were stained with DAPI (blue). Scale bars = 50 μ m. Yellow dotted lines in **B** and **C** indicated representative thyroid follicles. **D-F:** Immunofluorescence staining of the thyroid of an *Fgf10* $Ex1^{mut}/Ex3^{mut}$ chimeric neonate. **D:** A low magnification image acquired using a stereo fluorescence microscope. The thyroid of an *Fgf10*^{wild/wild} neonate placed on the same slide served as the control. White dotted lines indicate the thyroid glands. **E:** Image acquired using a confocal microscope (with slight magnification) of the tissue indicated by the yellow dotted box in **D**. Scale bars = 1 mm. T, trachea; C, cartilage; E, esophagus. **F:** Immunofluorescence staining of the thyroids of *Fgf10* $Ex1^{mut}/Ex3^{mut}$ neonates for GFP (green) and thyroid markers (red): TTF1, T3, Tg and Calcitonin. Nuclei were stained with DAPI (blue). Insets in **C** and **E** show magnified views of the areas indicated with white dotted lines. Scale bars = 50 μ m.

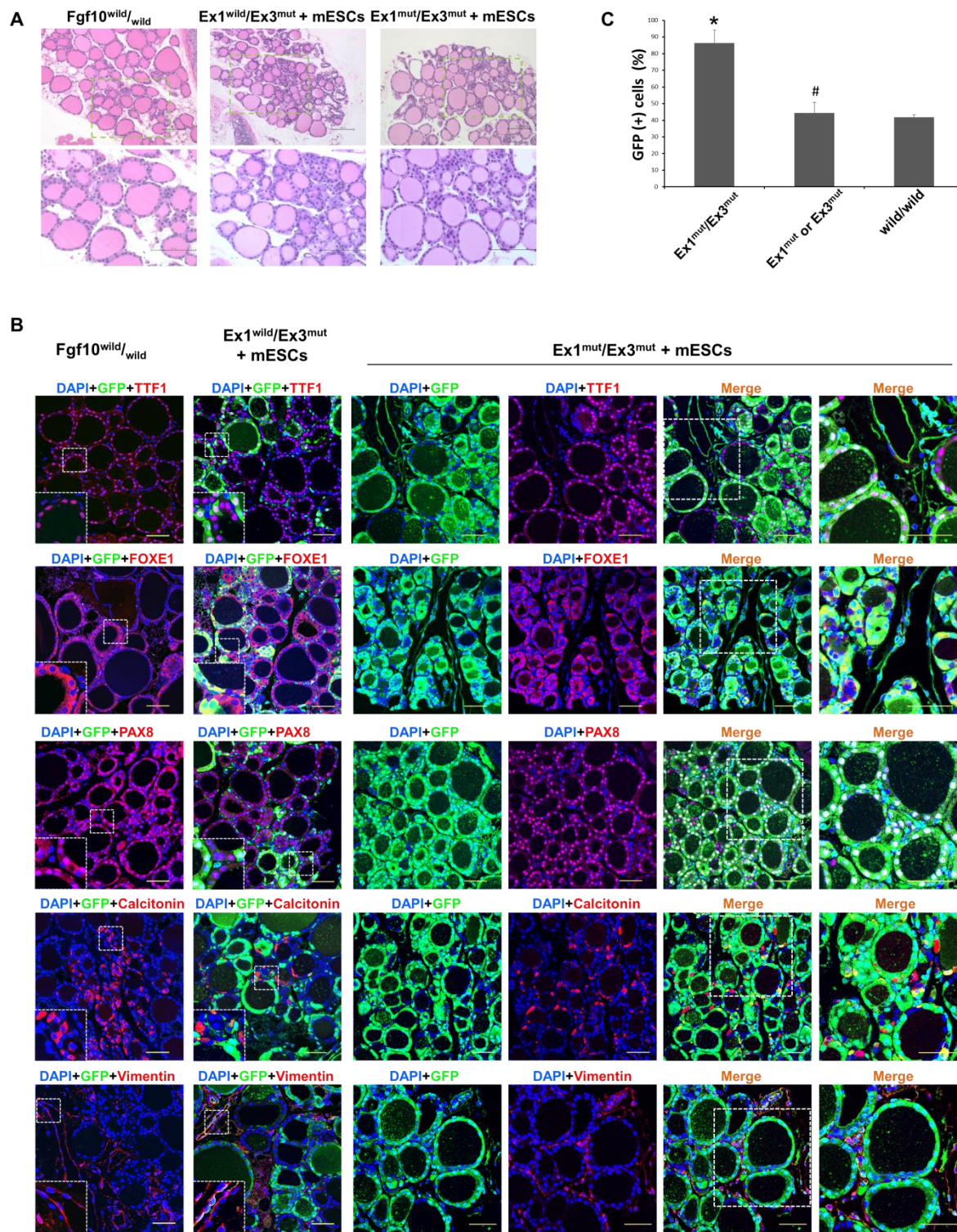


Figure 2. Characterization of the thyroids of adult *Fgf10* *Ex1*^{mut}/*Ex3*^{mut} chimeric mice complemented with mouse embryonic stem cells (mESCs). **A:** Hematoxylin and eosin staining of thyroid tissues from adult *Fgf10*^{wild/wild} mice, and *Fgf10* *Ex1*^{wild}/*Ex3*^{mut} and *Ex1*^{mut}/*Ex3*^{mut} chimeric mice. The bottom panels show magnified views of the areas indicated by the dotted lines in the top panels. **B:** Immunofluorescence staining of the thyroids of *Fgf10* *Ex1*^{mut}/*Ex3*^{mut} chimeric neonates for GFP (green) and various markers (red): TTF1, thyroid transcription factor 1; FOXE1, forkhead box E1; and PAX8, paired box gene 8 for follicular cells, Calcitonin for parafollicular cells, and Vimentin for stromal cells. Nuclei were stained with DAPI (blue). *Fgf10*^{wild/wild} and *Fgf10* *Ex1*^{wild}/*Ex3*^{mut} chimeric mice served as controls. Insets show magnified views of the areas indicated with white dotted lines. The right panels show magnified views of the areas indicated by the dotted lines in the left panels. Scale bars = 100 μ m for (A); 50 μ m for (B). **C:** Enumeration of GFP/TTF1-positive thyroid follicular cells in adult *Fgf10* *Ex1*^{mut}/*Ex3*^{mut}, *Fgf10* *Ex1*^{mut} or *Ex3*^{mut}, and *Fgf10*^{wild/wild} chimeric mice. Data are expressed as the means \pm standard deviations; n = 3/group. **p* < 0.05 versus other treatments; # *p* > 0.05 versus *Fgf10*^{wild/wild} chimeras.

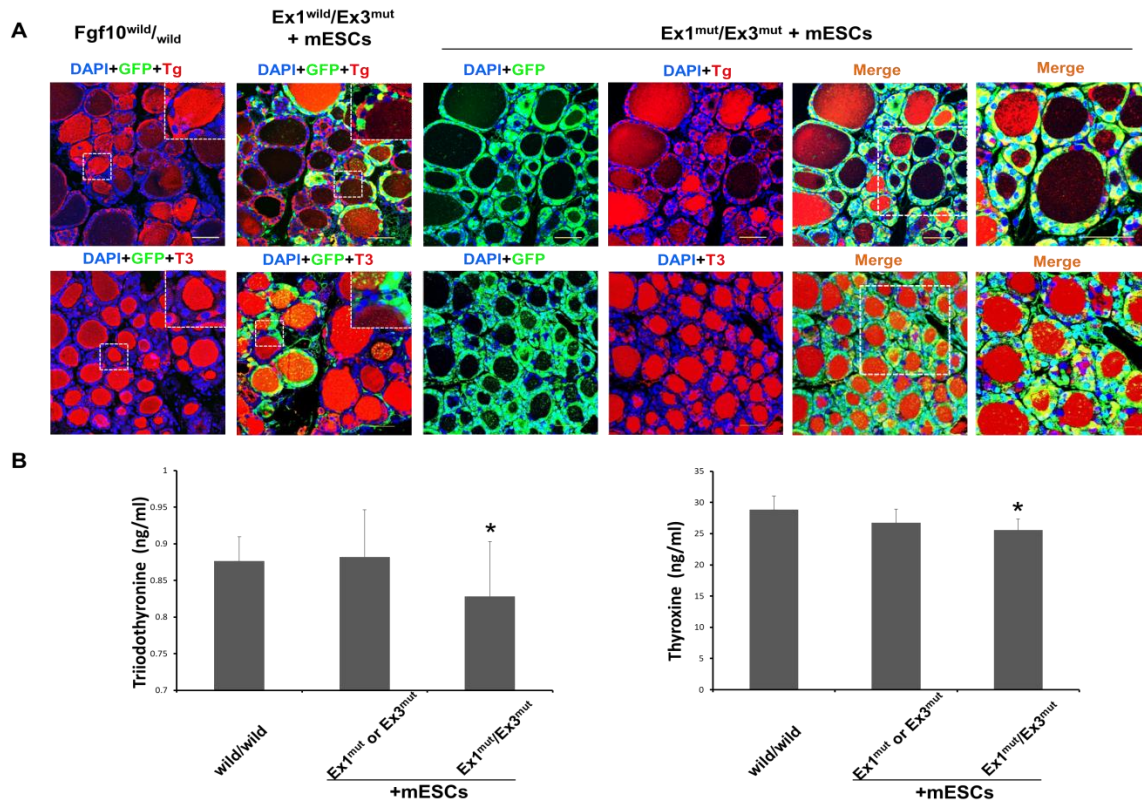


Figure 3. *In vivo* thyroid functionality assessment in adult *Fgf10* *Ex1*^{mut}/*Ex3*^{mut} chimeric mice complemented with mouse embryonic stem cells (mESCs). A: Immunofluorescence staining of the thyroids. Thyroid follicles were analyzed by staining for GFP (green) and markers of thyroid function. Tg, thyroglobulin; T3, tri-iodothyronine. Insets show magnified views of the areas indicated with white dotted lines. The right panels show magnified views of the areas indicated by dotted lines in the left panels. Nuclei were stained with DAPI (blue). *Fgf10*^{wild/wild} and *Fgf10*^{wild}/*Ex3*^{mut} chimeric mice served as controls. Scale bar = 50 μ m. **B:** ELISA analyses of serum tri-iodothyronine (T3) and thyroxine (T4) concentrations in adult *Fgf10* *Ex1*^{mut}/*Ex3*^{mut} chimeric mice. Adult *Fgf10*^{wild/wild} and *Fgf10* *Ex1*^{mut} or *Ex3*^{mut} chimeric mice served as controls. Data are expressed as the means \pm standard deviations; n = 3 for the adult *Fgf10* *Ex1*^{mut}/*Ex3*^{mut} chimeric mouse group and n = 4 for the adult *Fgf10*^{wild/wild} and *Fgf10* *Ex1*^{mut} or *Ex3*^{mut} chimeric mouse groups; *p > 0.05 versus other treatments.

The English in this document has been checked by at least two professional editors, both native speakers of English. For a certificate, please see:

<http://www.textcheck.com/certificate/YQt6qW>